

Electrochemical sensor for the determination of thiourea using a glassy carbon electrode modified with a self-assembled monolayer of an oxadiazole derivative and with silver nanoparticles

Masoud Rohani Moghadam¹ · Sanaz Akbarzadeh¹ · Navid Nasirizadeh²

Received: 17 October 2015 / Accepted: 9 December 2015 / Published online: 30 December 2015
© Springer-Verlag Wien 2015

Abstract This article reports on an electrochemical sensor for thiourea. It is based on a glassy carbon electrode (GCE) modified with a self-assembled monolayer of an oxadiazole derivative and with silver nanoparticles. The modified GCE demonstrated highly catalytic activity in terms of thiourea oxidation. The peak potential is shifted to negative values compared to a GCE coated with silver nanoparticles only. The electrode was characterized by linear sweep voltammetry, cyclic voltammetry and chronoamperometry, and thiourea was determined by differential pulse voltammetry in aqueous buffer of pH 7.0 resulting in two linear response ranges of 0.001–69.4 and 69.4–833.3 μM and the limit of detection of 0.1 nM. The method was applied to the determination of thiourea in copper refinery electrolyte, orange juice and tap water samples. The recoveries ranged from 96.9 to 108.0 %.

Keywords Copper electrorefining · Nanomaterial · Electrocatalytic oxidation · Differential pulse voltammetry · Linear sweep voltammetry · Chronoamperometry

Introduction

Thiourea (TU) as an organic additive is most commonly used in industrial processes of copper electrorefining from acidified copper sulfate solutions. Thiourea affects the structure of

deposited cathodes via the mechanism of electrolytic reduction processes. Smooth and pure copper is obtained in case the reagent is in a proper concentration. An insufficient amount of a smoothing reagent has an equally detrimental effect that causes the nodulation phenomenon of the cathode. Since thiourea is consumed during electrorefining by co-deposition with copper, it must be added to the electrolyte in a continuous way. Therefore, it is desirable to be able to measure the reagent concentration in the electrolyte [1, 2]. In food industries, TU is known as a toxic and hazardous, and these effects seem to arise from a disturbance of carbohydrate metabolism that may be harmful for humans. Furthermore, TU has also been screened as allergenic and carcinogenic factors [3].

Different analytical techniques such as UV–vis spectrophotometry [3, 4], UV reflectance spectrometry [5], infrared spectrometry [6, 7], chemiluminescence [8, 9], Raman spectroscopy [10], chromatography [11, 12] and electrochemical methods [1, 13–17] have been reported for the determination of thiourea in various samples. Electrochemical methods are suitable for determination of low levels of thiourea because of their high sensitivity and selectivity and inexpensive instrumentation. Development of various modified electrodes to achieve higher selectivity and sensitivity has been of interest, but there are few reports so far on the determination of thiourea using modifiers [17–20].

Nanomaterials have demonstrated special properties that are differing from bulk materials, originating from their quantum-scale dimensions. They have found wide applications in analytical methods [21, 22]. Different kinds of nanomaterials, such as metals, metal oxides, semiconductor nanoparticle and carbon-based materials have been used to fabricate electrochemical sensors

✉ Masoud Rohani Moghadam
masoud.rohani.moghadam@gmail.com

¹ Department of Chemistry, Faculty of Science, Vali-e-Asr University, 77188-97111 Rafsanjan, Iran

² Department of Textile and Polymer Engineering, Yazd Branch, Islamic Azad University, 89195-74 Yazd, Iran

and biosensors [23–25]. Metallic nanoparticle have significant ability to overcome some problems of modified electrodes such as low sensitivity, reproducibility and slow electron transfer. Silver exhibits the highest electrical and thermal conductivity among all metals. So, as compared to other metallic nanoparticles, silver nanoparticle (AgNP) may facilitate electron transfer and make it efficient in a better way [26]. In addition, remarkable catalytic properties of AgNP have made it a unique material to be used in modified electrodes [23].

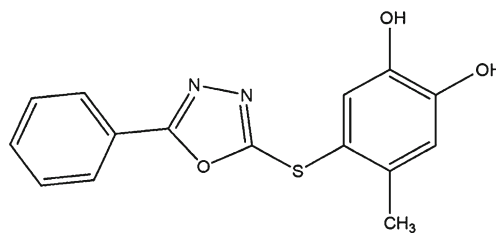
Oxadiazole and its derivatives, as S-functionalized compounds, have a strong tendency to be adsorbed onto the surface of silver particles. Such adsorption is used in preparing chemical interfaces with stable and structurally well-defined monolayers known as self-assembled monolayers (SAMs). These SAMs, as intermediate layers for accumulation and later reaction of target analytes, can enhance the selectivity and sensitivity of modified electrode surfaces. In addition, surface modifications using AgNP can largely increase the immobilized amount of oxadiazole and improve the stability of SAM layers [23, 27].

Direct oxidation of TU is limited by a substantial overpotential at conventional carbon electrodes. Besides, ordinary carbon electrodes have a low sensitivity and reproducibility as well as a slow electron transfer. One promising approach for lowering the overpotential to facilitate the determination of thiourea is to use electrocatalytic processes at chemically modified electrodes. One of the novel and beneficial methods to modify electrodes is utilization of nanotechnology for its advantages in decreasing potentials and achieving low detection limits. However, to our best knowledge, there is no report on AgNP modified glassy carbon electrodes (GCE) for determination of TU. In the present paper, we report the preparation of an oxadiazole derivative self-assembled layer on AgNP. Cyclic voltammetry, linear sweep voltammetry and chronoamperometry were used to investigate the electrocatalytic activity and electrochemical behavior of the modified electrode. Finally, the applicability of the modified electrode for determination of TU was demonstrated by analyzing the orange juice and electrolyte samples of National Iranian Copper Complex Industries using differential pulse voltammetry (DPV) technique.

Experimental

Materials and instruments

The oxadiazole derivative 4-((5-phenyl-1,3,4-oxadiazol-2-yl)thio)benzene-1,2-diol (Scheme 1) was prepared and purified as described [28]. Silver nitrate, nitric acid, and TU ($\text{SC}(\text{NH}_2)_2$) were



Scheme 1 Structure of the oxadiazole derivative

of analytical grades from Merck Company (www.merck.com/). A phosphate buffer (0.1 M) was supplied with H_3PO_4 , and the pH was adjusted using a 2.0 M NaOH solution. All the solutions were prepared with doubly distilled water. TU solutions were all prepared immediately prior to being used, and all the experiments were carried out at room temperature. All the test solutions were degassed by passing highly pure nitrogen (99.999 %) before the electrochemical experiments.

An Autolab potentiostat-galvanostat PGSTAT 30 (Eco Chemie, Utrecht, Netherlands) equipped with GPES 4.9 software (www.metrohm.com/), in connection with a three-electrode system and a personal computer was used for electrochemical measurements. The geometric area of the oxadiazole derivative silver nanoparticle-modified glassy carbon working electrode (QSNP-GCE) was 0.0314 cm^2 . A platinum electrode and a saturated calomel electrode (SCE) (Azar Electrode Co, Iran) (<http://company294.ecasb.com/en>) were used as the counter and reference electrodes respectively. All the potentials in the framework are given versus this reference electrode. The pH measurements were done with a Metrohm 827 pH/mV meter. Scanning electron microscopy (SEM) was done with a XL30 scanning electron microanalyzer (Philips's Company, Netherlands) (www.philips.com/) at an acceleration voltage of 20.0 kV.

Preparation of electrodes

Prior to modification, the bare GCE was polished consecutively with $0.05 \mu\text{m Al}_2\text{O}_3$ slurry on a polishing cloth and then rinsed with doubly distilled water. After that, the electrode was inserted in 1:1 nitric acid, absolute ethanol and doubly distilled water in an ultrasonic bath for 2 min.

To prepare the silver nanoparticle modified GCE (SNP-GCE), the bare GCE was immersed in a solution containing 100 mM nitric acid and 1.0 mM AgNO_3 , and a continuous cyclic potential was applied from -0.7 to $+1.9 \text{ V}$ at a sweep rate of 80 mV s^{-1} for 8 cycles [23]. Finally, the modified electrode was rinsed with doubly distilled water and dried in air.

The oxadiazole derivative modified GCE (OMGCE) was prepared by the self-assembling technique, just by placing $5.0 \mu\text{L}$ of a 1.0 mM oxadiazole derivative solution in a 0.1 M phosphate buffer (pH = 7.0) directly onto the GCE surface and drying it at room temperature without applying any

potential to the electrode. Finally, the modified electrode was rinsed thoroughly with distilled water. The procedure for preparation of the oxadiazole derivative modified silver nanoparticle-GCE (OSNP-GCE) was the same as the one used for OMGCE, but the oxadiazole derivative solution was placed, as described, onto the SNP-GCE.

Preparation of samples

Electrolyte samples of National Iranian Copper Complex Industries contain concentrated sulfuric acid (H_2SO_4) which causes damage to OSNP-GCE. So each sample was initially diluted for about 40 times with distilled water. Then, 100 mL of the sample solution was put in a proper baker containing a stirring bar. The pH meter and the magnetic stirrer were turned on, and the sodium hydroxide (NaOH) 2.0 M was added until the pH increased to about 7.0. Then, the solution was filtered with a filter paper, and the remaining solution was used as a prepared sample for the determination of TU.

On the other hand, the orange juice sample was collected by compressing fresh oranges. Then it was filtered through a filter paper (Schleicher & Schuell Ref. No. 10300112), and centrifuged for 15 min at 3500 rpm. After refluxing for 10 min and cooling, 25 mL of the solution was transferred into a 50 mL volumetric flask, and diluted to the mark with distilled water. 25 mL of this solution was transferred to a volumetric flask, diluted to 50 mL and analyzed using DPV technique [4].

Results and discussion

Characterization of the surface morphology of the OSNP-GCE

After the formation of an oxadiazole layer on the GCE surface, the surface morphologies of different electrodes were characterized by SEM, since the morphology was also related to the performance of the electrode. Figure 1 shows the morphologies of SNP-GCE (Fig. 1a) and OSNP-GCE (Fig. 1b). As it can be seen, the SEM of SNP-GCE displays a three-dimensional uniform structure. Figure 1b shows that OSNP-GCE has significant amount of oxidazole embedded in silver nanoparticle. In fact, when the oxidazole derivative is deposited in the OSNP-GCE, the bright particles of the oxidazole are observed (Fig. 1b). The aggregates of the deposited oxidazole molecules are distributed regularly and show an island-like structure.

Electrochemical behavior of OSNP-GCE

The cyclic voltammograms of OSNP-GCE in a 0.1 M phosphate buffer (pH=7.0) at various scan rates are shown in

Fig. 2. As shown in Fig. 2a, the ratio of cathodic-to-anodic peak currents obtained at various scan rates is almost constant. Furthermore, the cathodic and anodic currents increase linearly with the scan rate in the whole worked scan rate potentials (Fig. 2a) as predicted theoretically for a surface-immobilized redox couple. The linear dependence indicates that the nature of the redox process is diffusionless and controlled. The results show that the values of the anodic and cathodic peak potentials were proportional to the logarithm of the scan rate for scan rates higher than 2000 mV s^{-1} (Fig. 2b and c). At the potential scan rates of 5 to 1000 mV s^{-1} , the formal potential ($E^{0'}$) was constant due to the facility of charge transfer kinetics at this range.

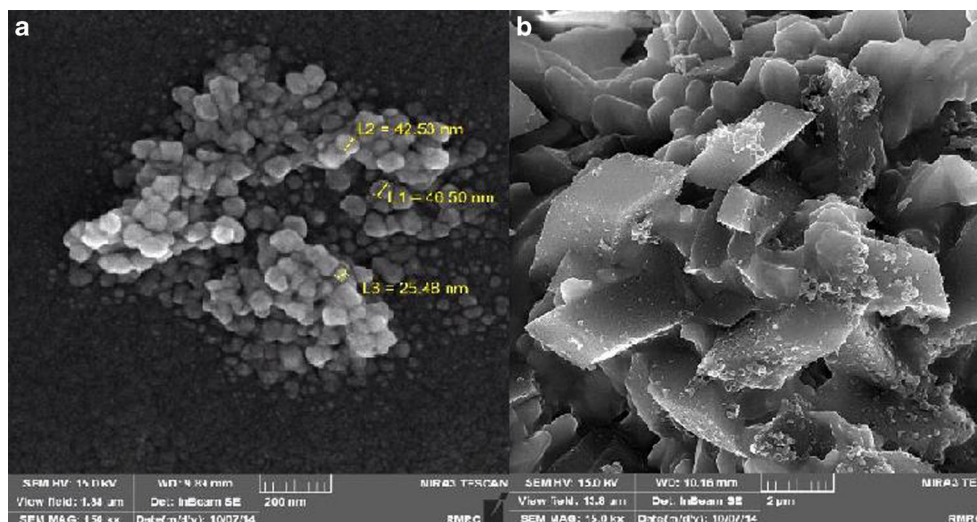
The formal potential ($E^{0'}$) value, which was obtained from the equation of $E^{0'} = E_{pa} - \alpha (E_{pa} - E_{pc})$ [29], is about 150 mV for sweep rates ranging from 5 to 1000 mV s^{-1} . According to the method described by Laviron [30], the electron transfer coefficient, α , as well as the heterogeneous rate constant, k_s , for the charge transfer between SNP-GCE and the oxadiazole derivative can be calculated from the slope of variation of E_p versus $\log(V)$. Inset B of Fig. 2 shows the variations of the peak potentials (E_p) as a function of the potential scan rate. The results show that the E_p values are proportional to the logarithm of the scan rate, for scan rates higher than 2000 mV s^{-1} (Fig. 2, inset C). Using the slope of plots in Fig. 2, inset C, the average values of $\alpha = 0.53$ and $k_s = 9.3 \pm 0.7 \text{ s}^{-1}$ were obtained at pH=7.0.

Electrochemistry of thiourea at OSNP-GCE

Cyclic voltammograms of OSNP-GCE (Fig. 3, curves a, b) without and with TU, SNP-GCE (Fig. 3, curve c), and OMGCE (Fig. 3, curve d) in the presence of TU were obtained in order to examine the potential electrocatalytic oxidation of TU using different modified electrodes.

In the absence of TU, an excellent redox peak couple of OSNP-GCE (curve a) can be observed. After addition of 0.1 mM of TU, as expected for electrocatalytic oxidation, an increase is observed in the anodic peak current of OSNP-GCE_{ox}/OSNP-GCE_{red} couple, so there is a decrease in its cathodic peak current (Fig. 3, curve b), that is probably due to the catalytic reaction mechanism. It is concluded that the best electrocatalytic effect for TU oxidation is gained at the OSNP-GCE surface. The oxadiazole derivative isn't immobilized on GC electrode and consequently no peak is observed in the related voltammogram (curve d). In addition, in the investigated potential range, no peak was indicated with SNP-GC in the presence of TU (curve c). Since the modifier has thiol group, have a strong tendency to be adsorbed onto the surface of silver particles via covalence bond. However, observation of the peak potential in the studied range (curves a, b), proves that modified electrode (OSNP-GCE) decreases the TU oxidation peak potential. This means that the combination of SNP and a

Fig. 1 SEM of (a) SNP–GCE and (b) OSNP–GCE



mediator (oxadiazole derivative) definitely improves the characteristics of TU oxidation and consequently increases the selectivity of the fabricated electrode for TU.

The effect of scan rates on the electrocatalytic oxidation of TU at OSNP–GCE was investigated by linear sweep voltammetry in a 0.1 M phosphate buffer (pH=7.0) containing 0.1 mM TU (Fig. 4).

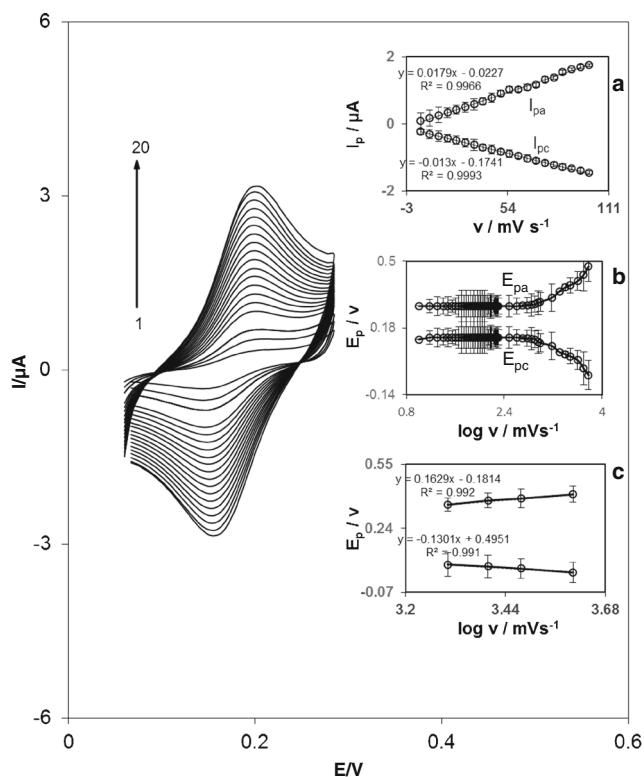


Fig. 2 Cyclic voltammograms of OSNP–GCE in 0.1 M phosphate buffer (pH=7.0) at different scan rates (The numbers 1–20 correspond to 5–100 mV s^{-1}). Insets: (a) plots of anodic and cathodic peak currents vs. of scan rate. (b) Variation of the peak potentials vs. the logarithm of the scan rate. (c) Magnification of the same plot for high scan rates

The oxidation peak current (I_p) of TU is proportional to the square root of the scan rate in the range of 8 to 12 mV s^{-1} (inset of Fig. 4a). This result implies that, at an adequate overpotential, the reaction is mass transport controlled while it is the best case for quantitative applications. From the slope of I_p versus $\nu^{1/2}$ plots, the approximate total number of electrons in the overall reaction can be calculated according to the following equation for a totally irreversible diffusion controlled process [31]:

$$I_p = 3.01 \times 10^5 n[(1-\alpha)n\alpha]^{1/2} A C_b D^{1/2} \nu^{1/2} \quad (1)$$

Where $D = (1.8 \pm 0.2) \times 10^{-5} \text{ cm}^2 \text{ s}^{-1}$ (diffusion coefficient of TU obtained by differential pulse voltammetry), $(1-\alpha)n\alpha = 0.61$, C_b is the bulk concentration of TU (mol cm^{-3}), and $A = 0.0314 \text{ cm}^2$ (the electrode surface area). It is estimated that the total number of electrons involved in the anodic oxidation of TU is 1.94~2. According to the results, the catalytic reaction

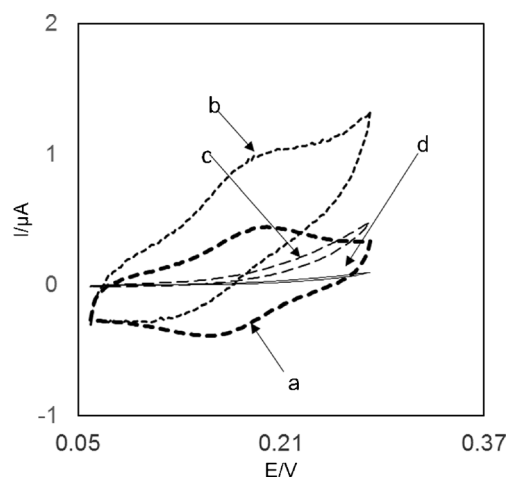


Fig. 3 Cyclic voltammogram of OSNP–GCE in the absence (a) and presence of 0.1 mM TU (b). Cyclic voltammograms of SNP-GCE (c) and OGCE (d) in the presence of 0.1 mM TU. Conditions: 0.1 M phosphate buffer (pH 7) at scan rate 20 mV s^{-1}

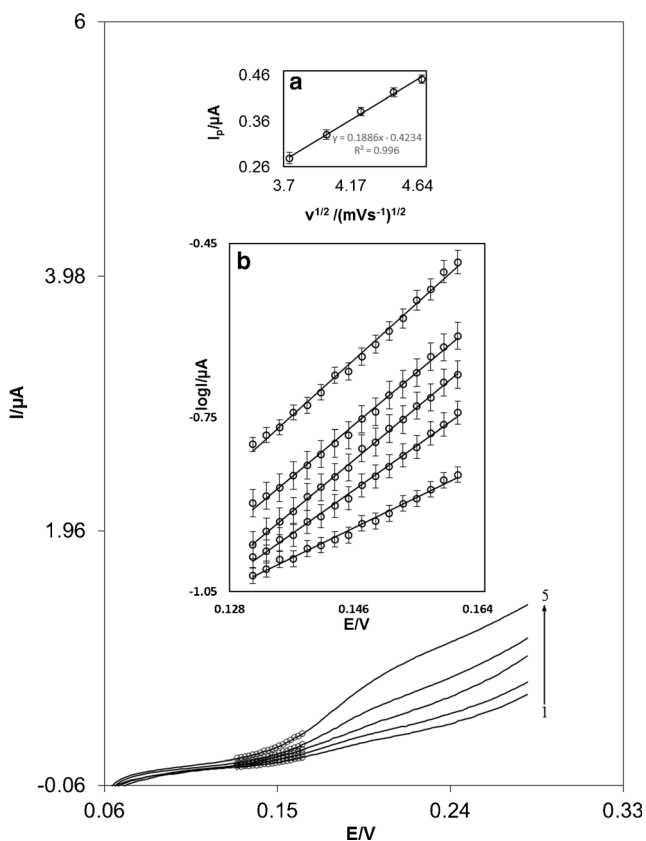
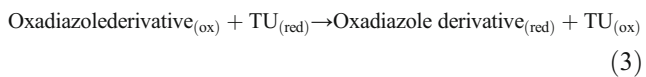
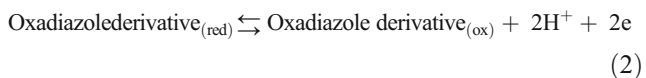
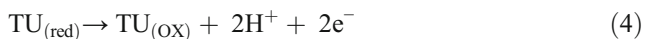


Fig. 4 Linear sweep voltammogram of OSNP-GCE in 0.1 M phosphate buffer (pH = 7.0) containing 0.1 mM thiourea at different scan rates (8–12 mV s⁻¹). Inset A shows variation of the electrocatalytic current versus the square root of scan rate. The points are the data used in the Tafel plots. Inset B shows the Tafel plots derived from the linear sweep voltammograms

(ErC_i') mechanism of TU at OSNP-GCE may be defined as shown in Eqs. 2 and 3. Based on these results, the following catalytic mechanism describes the voltammetric response of the electrocatalytic oxidation of TU at OSNP-GCE in a buffer solution pH = 7.0:



The overall oxidation of TU by the modified electrode is given in Eq. 4.



Under these conditions postulated for an ErC_i' mechanism, the catalytic rate constant between TU and oxadiazole derivative, k', is calculated based on Andrieux and Saveant theoretical model [32]. According to the model, the average value of k' was found to be (3.9 ± 0.05) × 10⁻³ cm.s⁻¹.

The linear sweep voltammograms of the modified electrode in a 0.1 M phosphate buffer (pH = 7.0) containing 0.1 mM of TU were obtained at the scan rates of 8, 10 and 12 mV s⁻¹ (Fig. 4b). In order to evaluate the information about the rate-determining step, the Tafel plots were drawn (inset of Fig. 4b) using points of the Tafel region of the linear sweep voltammograms. The results of polarization studies for the electro-oxidation of TU at OSNP-GCE show that, for all the potential scan rates, the average anodic Tafel slopes of 0.39 V⁻¹ was obtained for the different plots. Referring to Eq. 5 [33], the mean Tafel slope of 0.39 V⁻¹ concurs well with the contribution of two electrons in the rate-determining step of the electrode process, supposing a charge transfer coefficient of α = 0.39.

$$\text{Tafel slope} = (1 - \alpha)n_{\alpha} F / 2.3RT \quad (5)$$

It is necessary to mention that, according to the literature, the number of electrons elaborated in the rate-determining step of various processes is two. In addition, the exchange current density, J₀, is obviously readily accessible from the intercept of the Tafel plots. The average value of the exchange current density, J₀, for TU oxidation at the modified electrode surface was found to be 0.5 ± 0.1 μA cm⁻².

Chronoamperometric studies

The catalytic oxidation of TU by a SNP modified glassy carbon electrode was investigated by the chronoamperometry technique, in which the diffusion coefficient of TU was determined at the sensor surface. The chronoamperograms of OSNP-GCE in a 0.10 M phosphate buffer (pH = 7.0) containing different concentrations of TU obtained at the potential step of 250 mV are shown in Fig. 5. For an electroactive material (thiourea) with a diffusion coefficient, D, the current corresponding to the electrochemical reaction (under diffusion control) is defined by Cottrell equation [33]:

$$I = nFAD^{1/2}C/\pi^{1/2}t^{1/2} \quad (6)$$

Where D and C are the diffusion coefficient (cm² s⁻¹) and the bulk concentration (mol cm⁻³) of the analyte respectively. Figure 5a shows the tentative plots of I against t^{-1/2} for different concentrations of TU employed in the experiments. The slopes of the resulting straight lines were then plotted versus the TU concentration (inset B) from whose slope we found a diffusion coefficient of (1.8 ± 0.2) × 10⁻⁵ cm² s⁻¹ for TU.

Differential pulse voltammetric detection of thiourea at an OSNP-GCE

Differential pulse voltammetric, DPV, measurements were done to determine the linear range and to estimate the

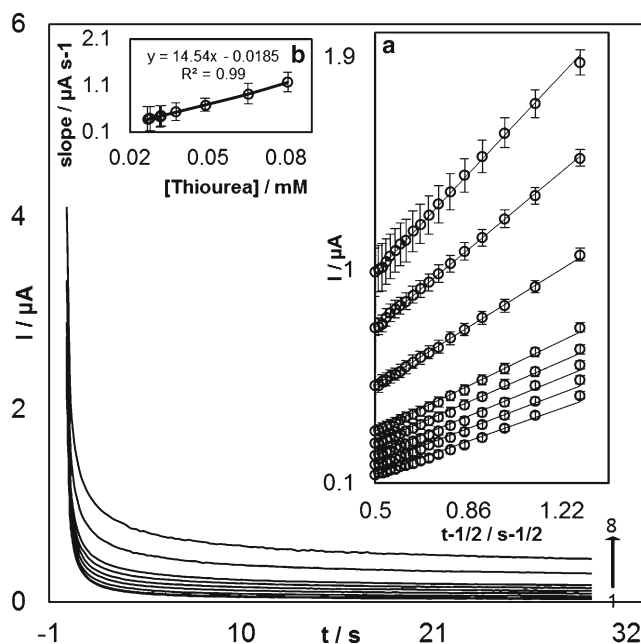
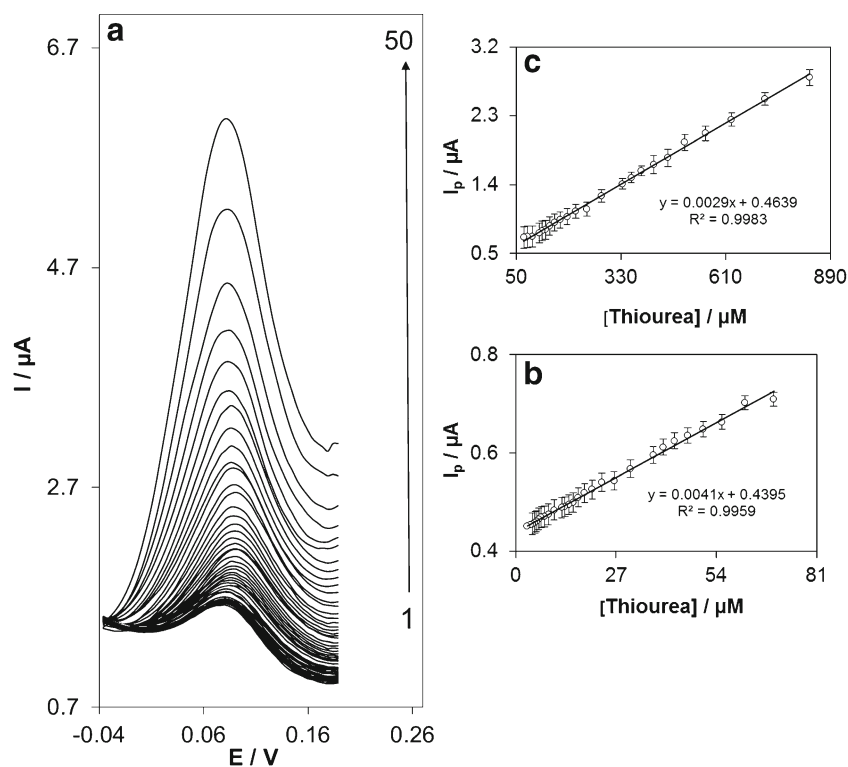


Fig. 5 Chronoamperometric response of the OSNP-GCE in 0.1 M phosphate buffer (pH=7.0) at potential step of 250 mV for different concentrations of thiourea. The numbers 1–8 correspond to 0.02, 0.04, 0.06, 0.08, 0.1, 0.2, 0.4, 0.6, 0.8 and 1 mM of thiourea. Insets: (a) plots of I versus $t^{-1/2}$ obtained from the chronoamperograms and (b) plot of the straight lines against the thiourea concentration

detection limit of TU at the introduced sensor. The voltammograms obtained for different concentrations of TU are depicted in Fig. 6a. As it is shown, DPV voltammograms from 0.000 to 0.150 V plotted and the related thiourea oxidation peak

Fig. 6 Differential pulse voltammograms of the OSNP-GCE in 0.1 M phosphate buffer (pH=7.0) containing different concentrations of thiourea (from 0.0 to 0.15 V and peak potential of 0.086 V). The voltammograms correspond to 0.001 to 833.3 μM thiourea. Inset A shows the plots of the electrocatalytic peak current as a function of thiourea concentration in the range of 0.001 to 69.4 and inset B is the peak current as a function of thiourea concentration in the range of 69.4 to 833.3



current on the surface of OSNPs-GCE was at 0.086 V (peak potential). The voltammograms are in the TU concentration ranges of 0.001–69.4 μM (Fig. 6b) and 69.4–833.3 μM (Fig. 6c). The slope (m) of the calibration plot in the first linear range (Fig. 5b) was used to estimate the detection limit of TU at the sensor by practicing the equation $C_m = 3s_{bl}/m$, where s_{bl} is the standard deviation of the blank response and m is the slope of the calibration plot. By analyzing these data, the limit of detection of TU was estimated to be 0.1 nM. The DPVs average current and the measurement precision shown by the relative standard deviation (RSD %) in ten repeated measurements ($n=10$) of an aqueous sample containing 40 μM of TU on OSNP-GCE were found to be $0.60 \pm 0.02 \mu\text{A}$ and 3.3 % respectively. Furthermore, in order to study the stability of the modified electrode, several OSNP-GCEs have been produced with the method described in the experimental part. Then the aforementioned modified electrodes were examined in the temporal range of 1 to 12 days with the conditions explained in the experimental section. The results have shown that the modified electrodes have the best stability for less than 5 days, and after 5 days, the electrodes response show more than 5 % decrease. In conclusion, the best stability of the modified electrodes is within 5 days storage, for the most effective use in measurements. It seems logical to claim that TU and its oxidation product(s) have no harsh effect on the modified electrode surface. Hence, OSNP-GCE was found to have outstanding advantages such as fast response time, a good limit of detection, a comprehensive linear range and almost a stable response for TU determination.

Table 1 Tolerance limit of organic compounds and diverse ions on the determination of 10 nM TU

Foreign species	Molar ratio
Methanol, ethanol, glucose, fructose, citric acid, tartaric acid, urea	1000
Li ⁺ , Na ⁺ , K ⁺ , Cu ²⁺ , Co ²⁺ , Ni ²⁺ , Fe ²⁺	1000
SO ₄ ²⁻ , NO ₃ ⁻ , HCO ₃ ⁻	1000
Fe ³⁺	400
Cl ⁻ , F ⁻	200
Glue	50
Hydroxylamine	20
Hydrazine	5

Interference study

The selectivity of the method was evaluated for the determination of 10 nM of TU in the presence of different inorganic ions and organic species. A relative error of less than $\pm 5\%$ was considered to be within the range of the experimental error. The results of this

Table 3 Analytical results for determination of TU in real samples ($n = 3$) with OSNPs – GCE

Sample	Added (μM)	Found (μM)	RSD (%)	Recovery (%)
National Iranian Copper Complex Industries electrolyte solution	0	0.137	3.48	–
	0.100	0.245	3.08	108.0
	0.500	0.644	3.68	101.4
	0.750	0.864	4.54	96.9
Orange juice	2.000	2.129	3.49	99.6
	0	0.033	3.29	–
	0.400	0.459	4.08	106.5
Tap water	0.800	0.842	2.61	101.1
	0	N.D.	–	–
	0.150	0.155	3.99	103.3
	0.350	0.345	1.89	98.6

investigation have been summarized in Table 1. It can be seen that in the presence of the most inorganic cations and anions no significant influence has been observed on the determination of TU. However, the tolerance of the method to

Table 2 Some critical properties of this work with previous studies about determination of thiourea

Method	Linear range (μM)	LOD (μM)	Sample	Ref
Kinetic Spect.	0.1–154	0.1	Fruit juice, orange peel	[3]
Reflectance Spect.	–	1.3	Fruit	[5]
Kinetic Spect.	0.38–128.01	0.003	Fruit juice, industrial waste water	[34]
UV–vis Spect.	97–768	11	Orange juice, lemon juice, orange peel	[35]
UV–vis Spect.	3–75	–	–	[36]
UV–vis Spect.	1.28–166.41	0.40	Tap water, orange juice, orange peel	[37]
IR Spect.	5.62×10^4 – 1.03×10^6	–	Gold leaching	[6]
IR Spect.	77–1016	13	Radiology film	[7]
Chemiluminescence	–	0.4	Wine	[8]
Chemiluminescence	0.04–4.00	0.003	Orange juice	[9]
Raman Spect.	3.8×10^4 – 2.6×10^5	–	Gold leaching	[10]
LC/UV	$<3.90 \times 10^3$	0.02	Industrial waste water	[11]
HPLC/UV	1.3–191.7	0.7×10^3	Flour	[12]
Electrochemistry	3.2×10^{-5} –1.8	3.2×10^{-5}	Cattle feed, urine	[13]
Electrochemistry	<1000	1	–	[14]
Electrochemistry	2.6–66	–	Copper refinery electrolytes	[15]
Electrochemistry	0.010–0.100	0.025	Waste water	[16]
Electrochemistry	100–1000 500–4000	20	Tap water	[18]
Electrochemistry	6.3–30	1.29	Waste waters	[19]
Electrochemistry	1–20	1	Fruit juices	[20]
Electrochemistry	–	0.26	Industrial waste water, fruit juice, orange peel	[17]
Electrochemistry	0.0025–140	0.09	–	[38]
Electrochemistry	1000–8000	–	Alkaline media	[39]
Electrochemistry	0.001–69.4 69.4–833.3	0.0001	Copper refinery electrolyte, orange juice, tap water	This work

some of the organic species, such as hydroxylamine and hydrazine is relatively low.

Comparison with other methods

The figures of merit of the present method for the determination of thiourea were compared with variety of analytical methods that reported previously (Table 2). As illustrated, the detection limit and linear range of the suggested modified electrode is significantly lower than those of the other reported methods (except [13]) and, consequently, analysis of the trace amounts of thiourea is possible by the introduced method in various samples.

Application

To examine the reliability of the recommended sensor, the method was applied for the determination of TU in the electrolyte sample of National Iranian Copper Industries, orange juice and tap water samples. In order to run the tests, 3.0 mL of a prepared samples was diluted to 10 mL with a 0.1 M phosphate buffer (pH = 7.0). Then, certain amounts of TU were added, and the responses of the sensor having OSNP–GCE as a working electrode were determined in differential pulse voltammetric measurements. The measurements were done using the calibration plots shown in Fig. 6. The accuracy of the method was verified by the analysis of the samples spiked with the known amounts of TU at different levels. As demonstrated in Table 3, the recoveries of added analyte are acceptable. These results indicate that the analyzed matrices have no effect on OSNP–GCE to determine TU and the introduced method can be used in various real samples.

Conclusion

This study confirmed that a recently synthesized oxadiazole derivative can be immobilized easily on the surface of a silver nanoparticle (SNP) modified glassy carbon electrode (GCE). As the results suggest, the reversibility of oxadiazole derivative and its electrocatalytic activity for TU oxidation are expressively improved when an OSNP–GCE is used instead of an OMGCE or SNP–GCE. According to the data in this study, the diffusion coefficient of TU was found to be $1.8 \pm 0.2 \times 10^{-5} \text{ cm}^2 \text{ s}^{-1}$ for experimental conditions using chronoamperometry results. In differential pulse voltammetric measurements, a limit of detection of 0.1 nM and two linear ranges were obtained for TU at the prepared modified electrode. Technical simplicity, high sensitivity, low detection limit and wide linear concentration ranges for TU are the great advantages of the modified electrode. Finally, it emerged that the DVP technique can be used to determine TU in the

electrolyte samples of National Iranian Copper Complex Industries, as well as orange juice and tap water samples. To this end, the prepared modified electrode has proved to be of benefit.

Compliance with ethical standards The authors declare that they have no competing interests.

References

1. Krzewska S, Pajdowski L, Podsiadly H, Podsiadly J (1984) Electrochemical determination of thiourea and glue in the industrial copper electrolyte. *Metall Trans* 15:451–459
2. Suarez D, Olson F (1992) Nodulation of electrodeposited copper in the presence of thiourea. *J Appl Electrochem* 22:1002–1010
3. Abbasi S, Khani H, Hosseinzadeh L, Safari Z (2010) Determination of thiourea in fruit juice by a kinetic spectrophotometric method. *J Hazard Mater* 174:257–262
4. Hosney R, Finney K (1964) Spectrophotometric determination of urea, thiourea, and certain of their substitution products with p-dimethylaminobenzaldehyde and diacetylmonoxime. *Anal Chem* 36:2145–2148
5. Mandrou B, Brun S, Kingate A (1977) Quantitative determination of thiourea in citrus fruits. *J Assoc Off Ana Chem* 60:699–701
6. Kargosha K, Khanmohammadi M, Ghadiri M (2001) Fourier transform infrared spectrometric determination of thiourea in the presence of sulphur dioxide in aqueous solution. *Anal Chim Acta* 437: 139–143
7. Kargosha K, Khanmohammadi M, Ghadiri M (2001) Vapour phase fourier transform infrared spectrometric determination of thiourea. *Analyst* 126:1432–1435
8. Li WH, Wang YZ (2006) Determination of thiourea by flow injection with chemiluminescence. *Physical testing and chemical analysis (Part B: Chemical Analysis)* 42:111
9. Fan X, Wang S, Chen F, Wang X (2012) FI-Chemiluminescence determination of thiourea [J]. *Physical Testing and Chemical Analysis (Part B: Chemical Analysis)* 12:31
10. Bowley HJ, Crathorne EA, Gerrard DL (1986) Quantitative determination of thiourea in aqueous solution in the presence of sulphur dioxide by Raman spectroscopy. *Analyst* 111:539–542
11. Rethmeier J, Neumann G, Stumpf C, Rabenstein A, Vogt C (2001) Determination of low thiourea concentrations in industrial process water and natural samples using reversed-phase high-performance liquid chromatography. *J Chromatogr A* 934:129–134
12. Li X, Wang J, Zhao Z, Wu G, Pang Y (2009) Determination of thiourea in flour by high performance liquid chromatography [J]. *Sci Technol Food Ind* 5:99
13. Stara V, Kopanica M (1984) Adsorptive stripping voltammetric determination of thiourea and thiourea derivatives. *Anal Chim Acta* 159:105–110
14. Pápay M, Tóth K, Pungor E (1971) Potentiometric determination of thiourea with a sulphide-selective membrane electrode. *Anal Chim Acta* 56:291–296
15. Akeneev YA, Zakharova EA, Slepchenko GB, Pikula NP (2005) Voltammetric determination of thiourea in copper refinery electrolytes. *J Anal Chem* 60:514–517
16. Spataru N, Spataru T, Fujishima A (2005) Voltammetric determination of thiourea at conductive diamond electrodes. *Electroanal* 17: 800–805
17. Tian L, Gao Y, Li L, Wu W, Sun D, Lu J, Li T (2013) Determination of thiourea using a carbon paste electrode decorated with copper oxide nanoparticles. *Microchim Acta* 180:607–612

18. Corb I, Manea F, Radovan C, Pop A, Burtica G, Malchev P, Picken S, Schoonman J (2007) Carbon-based composite electrodes: preparation, characterization and application in electroanalysis. *Sensors* 7:2626–2635
19. Levent A, Keskin E, Yardım Y, Şentürk Z (2011) Electrooxidation of thiourea and its square-wave voltammetric determination using pencil graphite electrode. *Rev Anal Chem* 30:45–51
20. Sezgintürk MK, Dinçkaya E (2010) Development of a biosensor for controlling of thiourea in fruit juices. *Food Bioprocess Tech* 3:128–134
21. Ríos A, Zougagh M, Bouri M (2013) Magnetic (nano) materials as an useful tool for sample preparation in analytical methods. A review. *Anal Methods* 5:4558–4573
22. Khodaveisi J, Dadfarnia S, Haji Shabani AM, Rohani Moghadam M, Hormozi-Nezhad MR (2015) Artificial neural network assisted kinetic spectrophotometric technique for simultaneous determination of paracetamol and p-aminophenol in pharmaceutical samples using localized surface plasmon resonance band of silver nanoparticle. *Spectrochim Acta A* 138:474–480
23. Nasirizadeh N, Aghayizadeh MM, Bidoki M, Yazdanshenas ME (2013) A novel sensor of quinazolin derivative self-assembled monolayers over silver nanoparticle for the determination of hydroxylamine. *Int J Electrochem Sci* 8:11264–11277
24. Goyal RN (2015) Gold nanoparticles decorated poly-melamine modified glassy carbon sensor for the voltammetric estimation of domperidone in pharmaceuticals and biological fluids. *Talanta* 141: 53–59
25. Van Hieu N, Duc NAP, Trung T, Tuan MA, Chien ND (2010) Gas-sensing properties of tin oxide doped with metal oxides and carbon nanotubes: a competitive sensor for ethanol and liquid petroleum gas. *Sensor Actuat B-Chem* 144:450–456
26. Narang J, Chauhan N, Jain P, Pundir CS (2012) Silver nanoparticle/multiwalled carbon nanotube/polyaniline film for amperometric glutathione biosensor. *Int J Biol Macromol* 50:672–678
27. Wang G, Wang W, Wu J, Liu H, Jiao S, Fang B (2009) Self-assembly of a silver nanoparticle modified electrode and its electrocatalysis on neutral red. *Microchim Acta* 164:149–155
28. Fakhari AR, Saeed Hosseiny Davarani S, Ahmar H, Hasheminasab K, Khavasi HR (2009) A facile electrochemical method for the synthesis of 5-phenyl-1,3,4-oxadiazol-2-ylthio-benzene-1,2-diol derivatives. *J Heterocyclic Chem* 46:443–446
29. Ju H, Shen C (2001) Electrocatalytic reduction and determination of dissolved oxygen at a poly (nile blue) modified electrode. *Electroanal* 13:789–793
30. Laviron E (1979) General expression of the linear potential sweep voltammogram in the case of diffusionless electrochemical systems. *J Electroanal Chem Interfacial Electrochem* 101:19–28
31. Nasirizadeh N, Zare HR (2009) Differential pulse voltammetric simultaneous determination of noradrenalin and acetaminophen using a hematoxylin biosensor. *Talanta* 80:656–663
32. Andrieux CP, Saveant JM (1978) Heterogeneous (chemically modified electrodes, polymer electrodes) vs. homogeneous catalysis of electrochemical reactions. *J Electroanal Chem Interfacial Electrochem* 93:163–168
33. Bard AJ, Faulkner LR (2001) Fundamentals and applications. *Electrochemical methods*, 2nd edn. Wiley, New York
34. Abbasi S, Khani H, Bagher Gholivand N, Naghipour A, Farmany A, Abbasi F (2009) A kinetic method for the determination of thiourea by its catalytic effect in micellar media. *Spectrochim Acta A* 72:327–331
35. de Oliveira AN, de Santana H, Zaia HCTBV, Zaia DAM (2004) A study of reaction between quinones and thiourea: determination of thiourea in orange juice. *J Food Compos Anal* 17:165–177
36. Kurzawa JK, Janowicz K (2005) Used of stopped-flow technique for investigation and determination of thiourea and its N-methyl derivatives as inducer for the iodine-azide reaction. *Anal Biol Chem* 382:1584–1589
37. Arab Chamjangali M, Goudarzi, Ghochani Moghadam A, Amin AH (2015) An on-line spectrophotometric determination of trace amounts of thiourea in tap water, orange juice, and orange peel samples using multi-channel flow injection analysis. *Spectrochim Acta A* 149:580–587
38. Zhang C, Jiang Y, Zhang D, Shan Y, Yang G (2015) Electrochemical determination of thiourea using thiophene derivatives-modified glassy carbon electrodes. *ECS Electrochem Lett* 4:B1–B3
39. Manea F, Radovan C, Schoonman J (2006) Amperometric determination of thiourea in alkaline media on a copper oxide–copper electrode. *J Appl Electrochem* 36:1075–1081